



Original Paper

Organic geochemistry and petrology of source rocks from the Banqiao Sag, Bohai Bay Basin, China: Implications for petroleum exploration



Xiang-Bai Liu ^{a, b}, Guang-Di Liu ^{a, b, *}, Wen-Ya Jiang ^c, Ze-Zhang Song ^{a, b}, Na Wang ^c

^a State Key Laboratory of Petroleum Resources and Prospecting, China University of Petroleum, Beijing, 102249, China

^b College of Geosciences, China University of Petroleum, Beijing, 102249, China

^c Exploration and Development Research Institute, Dagang Oilfield Company, PetroChina, Tianjin, 300280, China

ARTICLE INFO

Article history:

Received 16 September 2021

Received in revised form

25 February 2022

Accepted 12 July 2022

Available online 15 July 2022

Edited by Jie Hao

Keywords:

Lacustrine source rocks

Petrology

Biomarkers

Depositional environment

Banqiao Sag

ABSTRACT

The organic geochemistry and petrology of source rocks determine the hydrocarbon generation potential of the Banqiao Sag. In this study, organic geochemistry and petrology were used to determine the abundance of organic matter (OM), OM type, OM maturity, and sedimentary environments of the source rocks, collected from Cenozoic Shahejie Formation, Banqiao Sag, Bohai Bay Basin, China. Vitrinite and liptinite are the main maceral composition of the source rocks, and range from 18% to 81% and from 2% to 82% on a mineral matter free (MMF) basis, respectively. The values of vitrinite reflectance (R_o) (0.36%–1.20%) and the T_{max} values (397–486 °C) show that the thermal maturity range from low mature to peak-maturity. The abundance of OM varies between 0.22% and 4.37%, suggesting that the source rocks of the Shahejie (Es) Formation are mainly fair to good source rocks. The Rock-Eval pyrolysis results show that the source rocks have good petroleum generation potential. The amount of free hydrocarbons (S_1) and hydrocarbons generated from pyrolysis (S_2) range within 0.01–3.70 mg/g, and 0.04–29.17 mg/g. The hydrogen index (HI) varies between 18.18 and 741.13 mg HC/g TOC, with most of the samples appearing to be mainly Type II kerogen, and thereby exhibiting the ability to generate both oil and gas. The ratios of Pr/Ph, the cross plot of Pr/nC₁₇–Ph/nC₁₈, the cross plot of C₂₉/C₂₇–Pr/Ph, and ternary of dibenzothio- phene, dibenzofuran, and fluorene, indicate that the Shahejie Formation deposited in suboxic and weak reducing environments. The main biological source is from advanced plants. The maceral composition and rock pyrolysis data indicate the kerogen type is a humic type or mixed sapropelic-humic type. The source rocks of the Shahejie (Es) Formation occur in the oil window, and the abundant organic richness, humic kerogen demonstrate that these rocks are effective oil and gas source rocks. The mudstone rocks in the Shahejie Formation are the main source of oil and gas and represent the main exploration target for the Banqiao Sag. This study enhances the great prospect of oil and gas production in the Banqiao Sag. © 2022 The Authors. Publishing services by Elsevier B.V. on behalf of KeAi Communications Co. Ltd. This is an open access article under the CC BY-NC-ND license (<http://creativecommons.org/licenses/by-nc-nd/4.0/>).

1. Introduction

Banqiao Sag is a secondary structural unit in the north-central Huanghua Depression of the Bohai Bay Basin hinterland. The sag is in half-graben shape, which is faulted in the west part and overlapped in the east part with an individual area of about 540 km². Banqiao Sag is one of the most petroliferous sags and has been discovered significant proven oil reserves and undiscovered resources. More importantly, several oil and gas reservoirs have

been discovered in Banqiao Sag in the past 60 years. Although the level of exploration has improved in recent years, exploration has become more complicated, and whether can we find more resources have become the main factor restricting the exploration and development of oil and gas in this sag. The organic geochemistry and petrology of source rocks determine the hydrocarbon potential of a basin (Ding et al., 2015, 2016a, 2016b; Gao et al., 2016, 2017; Luo et al., 2016; Chen et al., 2020). In contrast, previous studies showed the characterisation of OM and the depositional environment of Banqiao Sag was limited and unknown. Most of the previous studies of Banqiao Sag were mostly based on pyrolysis methods (Chen and Wang, 2010), without research on biomarkers and petrology of source rocks. Biomarker distributions have been

* Corresponding author. State Key Laboratory of Petroleum Resources and Prospecting, China University of Petroleum, Beijing, 102249, China.

E-mail address: guangdiliucupb@gmail.com (G.-D. Liu).

used effectively to characterize the environmental conditions and source input of organic matter during the deposition (Brassell et al., 1978; Damsté et al., 1995; Hughes et al., 1995; Peters et al., 2005; Bechtel et al., 2012). The distribution and the organic geochemical characteristics of the source rocks are essential to determine the direction of petroleum exploration (Ding et al., 2015; Zhao et al., 2015). We have done a lot of research in organic geochemistry and petrology on the Cenozoic Shahejie Formation source rocks to investigate the origin and type of the OM, thermal maturity, oil/gas proneness and depositional environments of the source rocks in the Banqiao Sag. Through the above research, high precision and accuracy in oil and gas resource prediction and evaluation will be possible.

2. Geological setting

Banqiao Sag is a secondary structural unit in north-central Huanghua Depression, a secondary tectonic unit in Mesozoic-Cenozoic expanding areas of the Bohai Bay Basin hinterland. The Cangxian uplift bounds it to the northwest; the Beidagang buried hill to the southeast (Fig. 1). It extends from the Lvjuhe region into the Qikou Sag on the east and is a significant oil source sag in Huanghua Depression. The sag is in half-graben shape, which is faulted in the west part and overlapped in the east part with an individual area of about 540 km². Banqiao Sag is a typical Cenozoic continental facies basin, which has experienced three stages: the initial stage of rifting, the development of rifting and the decline of rifting (Cheng et al., 1999; Zhang et al., 2009; Sun et al., 2012; Ren et al., 2014; Song et al., 2015; Liu et al., 2017; Yang et al., 2019).

The sequences of the Banqiao Sag comprise the Neogene Minghuazhen (Nm), Guantao (Ng) formations, and the Paleogene Dongying (Ed), Shahejie (Es) formations (Guo et al., 2011) (Fig. 2). The Es Formation can be further divided into three members Es₃, Es₂, and Es₁, which are the primary hydrocarbon source rocks in the Banqiao Sag. Exploration in recent years has proven that the reservoir in Banqiao Sag is mainly distributed in Cenozoic formations, in which the reserves of Es₁ and Es₂ account for more than 80% (Li et al., 2004). Favorable oil and gas source conditions have laid an important foundation for oil and gas exploration in this area. Seven oil-bearing series, including Es, Ed, Ng, Nm formations, and lower Paleozoic Ordovician, have been found in the Banqiao Sag, as well as some oil fields and petroliferous structures. According to statistics, 81.79 million tons of accumulated proven oil reserves and

51.981 billion cubic meters of natural gas have been found (Liu et al., 2017).

3. Samples and experiment

All mudstone samples of the Shahejie Formation (Es), collected from drill core in the Banqiao Sag, were processed and in preparation for the total organic carbon (TOC) measurements and pyrolysis analysis. Moreover, 25 samples were selected for gas chromatography-mass spectrometry (GC-MS) analysis, 38 samples were used for vitrinite reflectance (R_o) measurements, 19 samples were selected for petrological analyses, and 20 samples were measured for the carbon isotope of organic matter.

The samples were pulverised to 100 mesh to prepare for the TOC measurement and Rock-Eval pyrolysis firstly. During the TOC testing, dilute hydrochloric acid was used to remove the inorganic carbon in the crushed samples. After that, the samples were repeatedly rinsed with distilled water until the solvent was neutral. Lastly, the samples were dried in an oven at 60–80 °C to prepare measurement using a LECO CS-230 analyzer. A Rock-Eval instrument is used to perform the pyrolysis analysis, which provides the parameters of T_{max} , S_1 and S_2 , and the results are listed in Table S1 (in Supplementary materials).

Soxhlet extraction method was used to extract OM from mudstones and chloroform/methanol (87:13) were employed for 72 h. Silica gel and alumina column chromatography was conducted to separate the isolated extractable organic matter into saturated hydrocarbons, aromatic hydrocarbons, nonhydrocarbon, and asphaltene. The saturated and aromatic fractions were analyzed by an Agilent 7890-5975c instrument. An HP-5MS fused silica column was equipped and ultrahigh purity He was used as the carrier gas at a flow rate of 1 mL/min. For analysis of the saturate fractions, the GC oven temperature was initially held at 50 °C for 1 min, then programmed to 120 °C at 20 °C/min, and to 250 °C at 4 °C/min, and to 310 °C at 3 °C/min, and held at 310 °C for 30 min. 290 °C was the temperature of the injector. The tricyclic terpanes and hopanes ($m/z = 191$), and steranes ($m/z = 217$) were monitored by the data acquisition system, which has selected ion monitoring capabilities. In order to calculate the relative abundances of triterpanes and steranes, the peak areas in the m/z 191 and m/z 217 fragmentograms were measured respectively. The results are listed in Tables S2 and S3 (in Supplementary materials).

The characteristics of maceral composition were analyzed on a

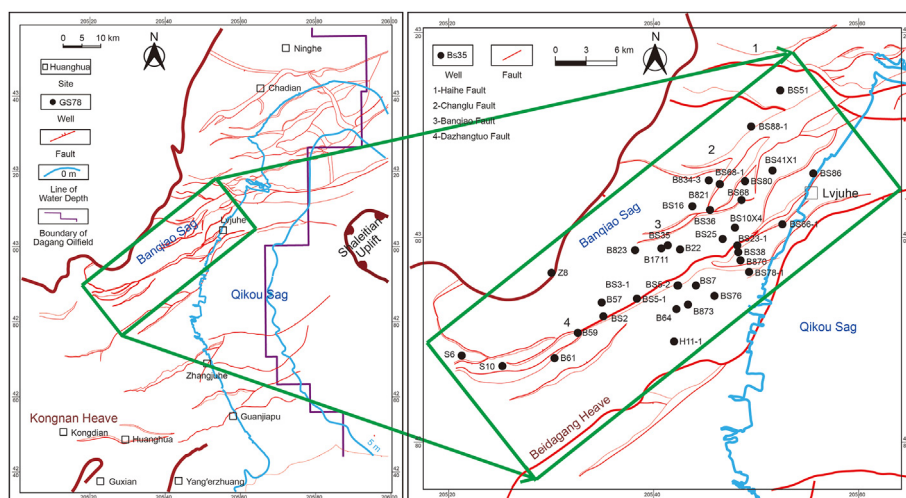


Fig. 1. Geologic map of Banqiao Sag, Bohai Bay Basin. The distribution of the samples in this study were marked by the green box.

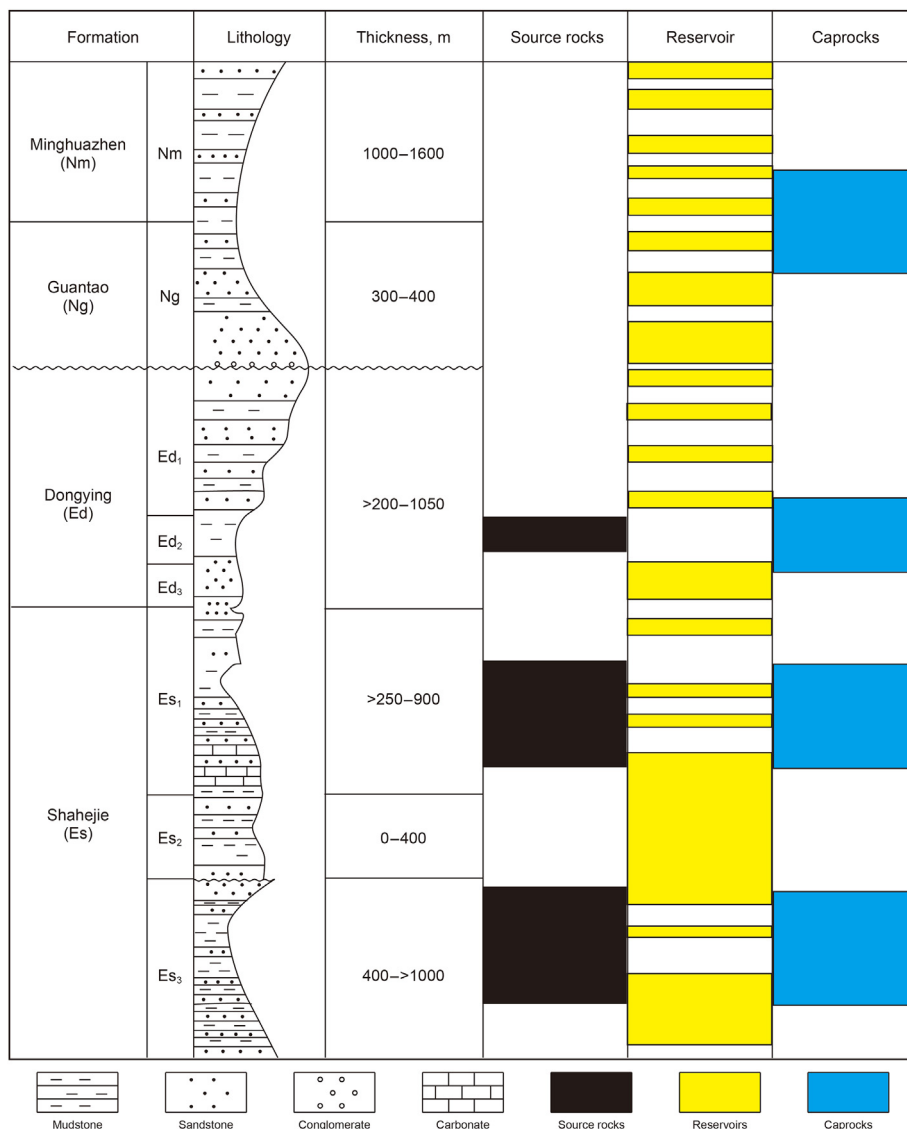


Fig. 2. Generalised stratigraphy and primary possible source rocks, major reservoir intervals, caprocks in the Banqiao Sag.

Leica microscope, equipped with the reflected fluorescent light and white light. The polished samples' random vitrinite reflectance (R_o) was measured by a Leica MPV Compact II reflected-light microscope with the oil immersion method. The vertical incident light was projected onto the samples and the intensity of the reflected light was measured. Compare the intensity with the reflection light intensity under the same conditions (humidity 35%, temperature 20 °C), on the premise of the reflection light intensity was measured on standard material with known reflectivity. The results are listed in Table 1 and S4 (Table S4 is in Supplementary materials). The carbon isotopic ratios were measured by a DELTA plus XL C003 based on the standard (GB/T18340.2–2010). Before the measurement, samples were treated with HCl and HF to remove carbonates and silicates. The results are listed in Table 2.

4. Results and discussion

4.1. Organic petrology

Maceral compositions data of the 19 studied samples are shown in Table 1. Vitrinite and liptinite particles derived from higher

plants are dominant and present as collinite, telinite, vitrodetrinite and exodetrinite. Under fluorescent light, exodetrinites display intense yellow and orange fluorescence. Vitrinites are mainly in the form of thin strips and debris (Fig. 3).

The percentages of vitrinite and liptinite within 18–81 vol% and 2–82 vol%, with an average of 58 vol% and 38 vol% on a mineral matter free (MMF) basis. The percentages of vitrinite are 18–65 vol% in Es₁ with an average of 47 vol%, 32–81 vol% in Es₃ with an average of 62 vol%. The percentages of liptinite are 35–82 vol% in Es₁ with an average of 52 vol%, 2–68 vol% in Es₃ with an average of 32 vol%. Small amounts of inertinite contents have been observed in several samples, and only in sample BS38, exceed liptinite contents (Table 1). The R_o in the samples from burial depth less than 3000 m are low, ranging from 0.36% to 0.45%. The R_o values are 0.36%–1.20% in Es₁ with an average of 0.82%, 0.52%–1.15% in Es₃, with an average of 0.76%, as listed in Table S4. Generally, R_o has a positive correlation (the fitting coefficient R^2 reaching 0.9082) with burial depth, and R_o increases with an increase in burial depth (Fig. 4). When the buried depth reaches about 2900 m, the organic matter reaches the low mature stage ($R_o = 0.5\%$).

Table 1
Maceral compositions of the Shahejie Formation mudstones.

Formation	Wells	Depth, m	V, %	L, %	I, %	S, %	TI
Es ₁	B57	2578.00	57	42	1	0	-23
	B64	2471.40	18	82	0	0	27
	B834-3	3140.30	65	35	0	0	-31
	B870	3066.50	4	40	1	55	70
	BS66-1	3748.70	53	43	4	0	-22
	S6	1958.30	43	57	0	0	-4
	Z8	3014.90	57	34	9	0	-35
Es ₂	S10	2340.00	54	46	0	0	-17
Es ₃	B38	3640.30	68	2	30	0	-79
	B59	3117.30	62	33	6	0	-36
	B59	3493.20	66	28	6	1	-40
	B59	3703.30	73	16	11	0	-57
	B61	3274.60	32	68	0	0	10
	BS2	3613.00	67	29	4	0	-39
	BS2	3905.00	81	19	0	0	-51
	BS35	3955.70	65	30	5	0	-39
	BS51	3574.00	41	59	1	0	-2
	BS5-2	3687.50	71	23	6	0	-48
	BS88-1	4097.30	54	45	2	0	-20

Abbreviations: V, Vitrinite; L, Lipitinite; I, Inertinite; S, Sapropelinite; TI, Type index.

Table 2
The carbon isotopic ratios of the organic matter in Shahejie Formation mudstones.

Formation	Wells	Depth, m	$\delta^{13}C_{org}$, ‰	Formation	Wells	Depth, m	$\delta^{13}C_{org}$, ‰
Es ₁	B57	2578.00	-25.2	Es ₃	B59	3703.30	-25.0
	B64	2471.40	-27.7		B61	3274.60	-24.3
	B834-3	3140.30	-25.3		BS2	3613.00	-24.6
	B870	3066.50	-27.2		BS2	3905.00	-25.1
	BS66-1	3748.70	-24.3		BS35	3955.70	-23.7
	S6	1958.30	-26.0		BS38	3640.30	-25.1
	Es ₂	B59	3117.19		-24.9	BS51	3574.00
S10		2340.00	-22.4		BS5-2	3687.50	-22.4
Z8		3014.86	-23.0		BS88-1	4097.30	-23.9
Es ₃	B59	3493.20	-21.6		H11-1	3598.90	-22.8

4.2. Organic geochemistry

4.2.1. TOC and rock pyrolysis

The organic matter abundance of source rocks is evaluated by TOC commonly, and the fundamental to hydrocarbon generation in source rocks is the OM (Mulier, 2002; Kao et al., 2004). Besides, hydrocarbon generation potential (S_1+S_2), bitumen content, and total hydrocarbon (HC) are used in evaluating the OM abundance of source rock (Tissot and Welte, 1978; Hunt, 1979; Huang et al., 1984; Cheng et al., 1995). In the Banqiao Sag, the TOC contents of mudstone samples show a wide range of 0.22%–4.37% (average = 1.30%). The results of 127 samples show that TOC in Es₁ is a little higher than that of Es₃, except for those with TOC less than 0.4. The average value of TOC contents of Es₁ is 1.47%, while the Es₃ with TOC contents averaging 1.21%. In detail, the TOC ranges within 0.3%–1.0% are more than 50% (53.09%) in Es₃, while that in Es₁ are only 46.88%. By comparison, the TOC content of Es₁ exceeding 2.0% is flat for that of Es₃ (Fig. 5).

Rock-Eval pyrolysis method is often used to classify OM types and evaluate the generating potentials of hydrocarbon. The studied samples have hydrogen index (S_2/TOC) of 18.18–741.13 mg HC/g TOC in the Banqiao Sag, which shows the source rocks' kerogen composition are in type I to type III in Shahejie Formation, and type II₁, II₂ are the main type. The amount of S_1 is lower in Es₁ than that in Es₃. In contrast, the S_2 of the kerogen and S_1+S_2 are higher in Es₁ than that in Es₃, ranging from 0.01 to 3.70 mg HC/g rock, 0.04–29.17 mg HC/g rock, and from 0.13 to 29.75 mg HC/g rock, respectively. In detail, the $S_1, S_2, (S_1+S_2)$ range within 0.01–0.92 mg/g, 0.14–29.17 mg/g, 0.16–29.75 mg/g with an average of 0.21 mg/g, 6.37 mg/g, 6.58 mg/g in the Es₁ mudstone samples and within

0.04–1.98 mg/g, 0.04–16.31 mg/g, 0.13–16.93 mg/g with an average of 0.48 mg/g, 3.10 mg/g, 3.58 mg/g in the Es₃ mudstone samples, respectively (Table S1). The TOC and S_2 are positively correlated, and the fitting coefficient R^2 is 0.9564 in the Es₁ and 0.8473 in the Es₃ mudstones (Fig. 6, kerogen classification standard from Wang et al., 2015). The slope of the line, which denotes the hydrogen index ($HI = S_2/TOC \times 100$), of the Es₁ mudstone samples (776 mg/g) is steeper than that of the Es₃ mudstone samples (477 mg/g), indicating the OM in the Es₁ mudstone samples is more oil-prone. The TOC versus ($S_1 + S_2$) plot showing that the mudstones are mainly fair-good source rocks (Fig. 7, maturation scale from Lu et al., 2008).

The studied samples have T_{max} values in the range of 397–486 °C, indicating the low to high maturity OM of source rocks (Table S1).

4.2.2. Carbon isotopic composition of organic matter

The $\delta^{13}C_{org}$ (‰) values show a wide range of -27.7‰ to -21.6‰ (average = -24.5‰), and have some variation in different formations. In detail, the $\delta^{13}C_{org}$ values in the Es₁ mudstones range from -27.7‰ to -24.3‰, with an average of -26.0‰. The $\delta^{13}C_{org}$ values in the Es₂ and Es₃ mudstones are similar, ranging from -24.9‰ to -22.4‰ (average = -23.4‰), and from -25.1‰ to -21.6‰ (average = -23.9‰), respectively (Table 2).

4.2.3. Aliphatic hydrocarbons

The mudstones extracts from Shahejie Formation (Es) contain a full range of C₁₂–C₄₀ n-alkanes, pristane, phytane, isoprenoids (Fig. 8). Most of the n-alkane patterns are dominated by short (C₁₅–C₂₀) to middle (C₂₁–C₂₃) chain n-alkanes, and only several

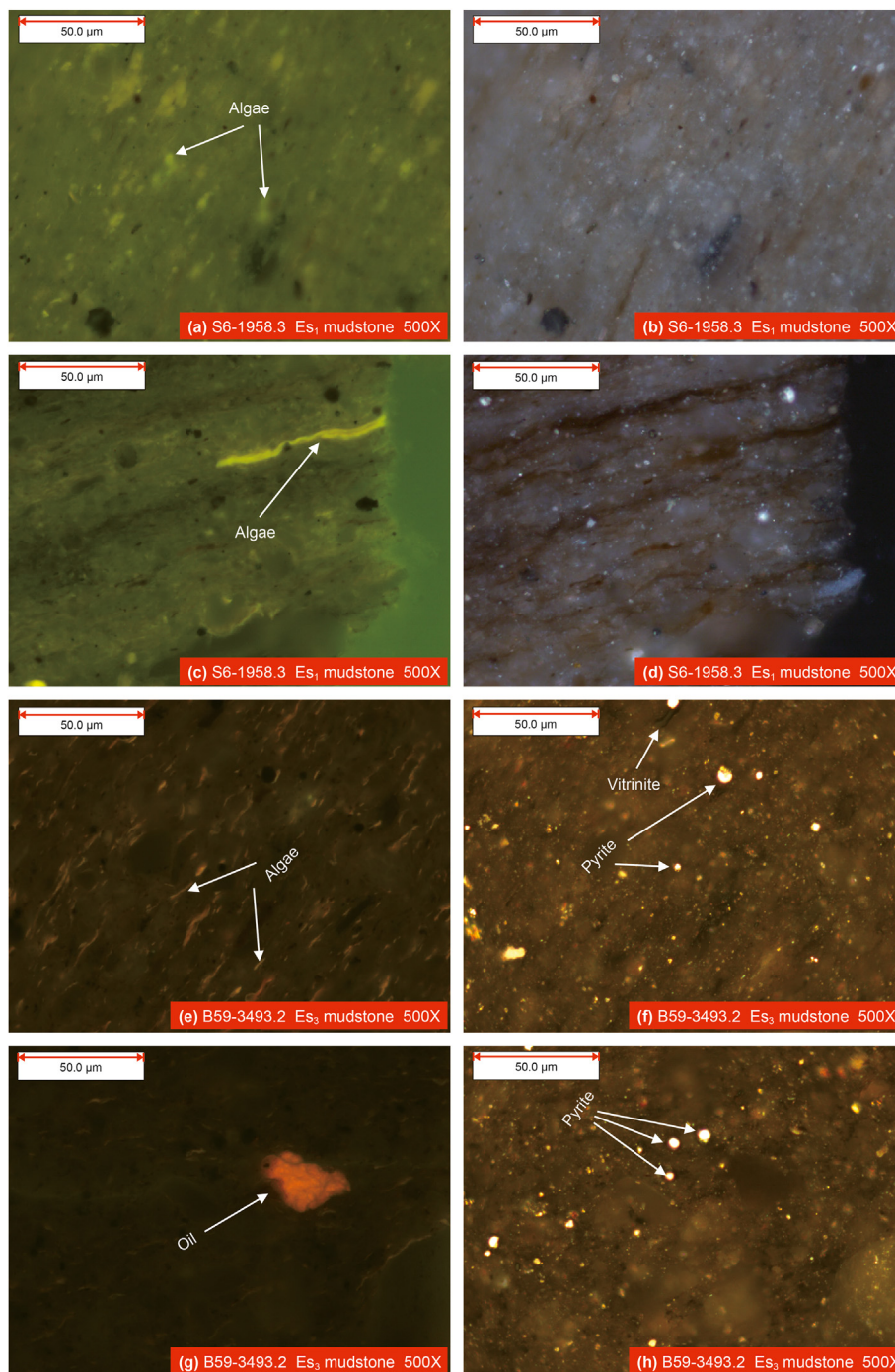


Fig. 3. Photographs of the maceral compositions in the Shahejie Formation: (a)(c) features of vitrinite and inertinite under reflected light, mudstone, S6; (b)(d) same field as (a)(c), but in a fluorescence mode; (e)(g) features of vitrinite and inertinite under reflected light, mudstone, B59; (f)(h) same field as (e)(g), but in a fluorescence mode.

samples are dominated by long (C_{25} , C_{27}) chain n-alkanes (Table S2). The distribution of n-alkane in the Es_1 and Es_3 samples follows unimodal distribution with a maximum at C_{15} – C_{23} (Fig. 8).

Low molecular weight (LMW) homologues ($<C_{22}^+$) with high nC_{21}/nC_{22}^+ ratio have a strong advantage, ranging from 0.48 to 3.80 (average = 1.40), in most of the samples. (Table 1). In all samples, the CPI values greater than 1, ranging from 1.03 to 1.46 (average = 1.31). The high OEP values (average > 1) were tested in most of the samples. The high CPI values suggest that the source of OM was a mixture of photosynthetic organisms and terrestrial plants (Peters et al., 2005).

There are a large amount of acyclic isoprenoids (Fig. 8), and the concentrations of pristane (Pr) is higher than phytane (Ph), as the ratio of Pr/Ph (between 0.16 and 5.56, average = 1.80) reveals. The ratio of Pr/ nC_{17} and Ph/ nC_{18} occur from 0.27 to 3.15 and 0.14 to 5.41, respectively (Table 1).

All samples contain Ts, Tm, C_{29} , and C_{30} hopanes and moretanens, C_{30} diahopane, gammacerane, and C_{31} – C_{35} homohopanes (Fig. 8). The C_{29} $\alpha\beta/(\alpha\beta + \beta\alpha)$ and C_{30} $\alpha\beta/(\alpha\beta + \beta\alpha)$ hopane ratios range from 0.46 to 0.90 (average = 0.78) and 0.71 to 0.92 (average = 0.87), respectively. The C_{31} $22S/(22S + 22R)$ and C_{32} $22S/(22S + 22R)$ homohopane ratios range from 0.35 to 0.62 (average = 0.56) and

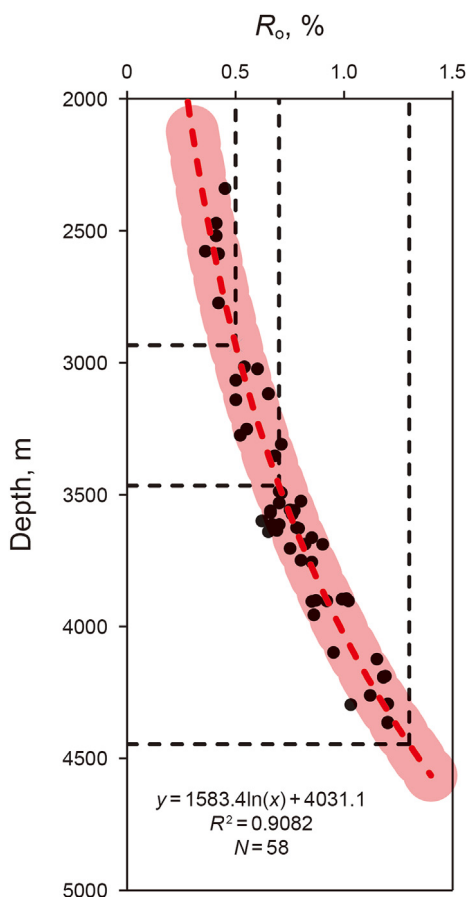


Fig. 4. Vitrinite reflectance (R_o) versus depth of Banqiao Sag, Bohai Bay Basin. N = number of samples.

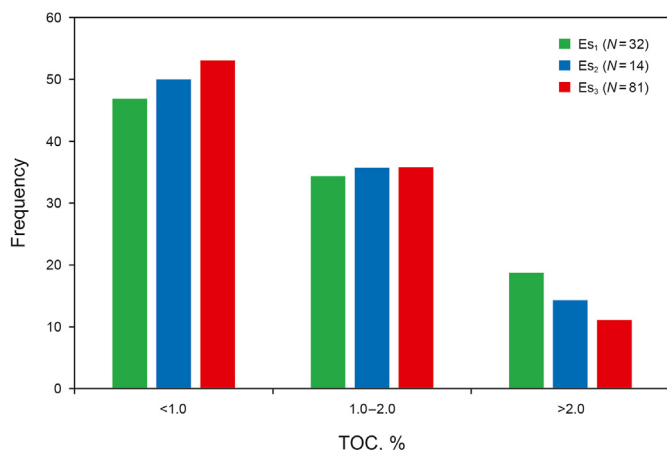


Fig. 5. Histograms of TOC in the mudstones of the Shahejie Formation. N = number of samples.

0.07 to 0.63 (average = 0.46), respectively. The low $Ts/(Ts + Tm)$ ratios (0.05–0.89) and $C_{29} Ts/(C_{29} Ts + C_{29} \alpha\beta \text{ hopane})$ (0.05–0.38) and low to high Gammacerane index (Gammacerane/ $C_{30} \alpha\beta \text{ hopane}$) (1.99–79.11, average = 17.25) has been determined in these samples. There is a wide distribution of $C_{29} \alpha\alpha\alpha 20S/(20S + 20R)$ and $C_{29} \alpha\beta\beta/(\alpha\beta\beta + \alpha\alpha\alpha)$ ratios in these samples, ranging from 0.04 to 0.73 and from 0.16 to 0.60, respectively (Table S3).

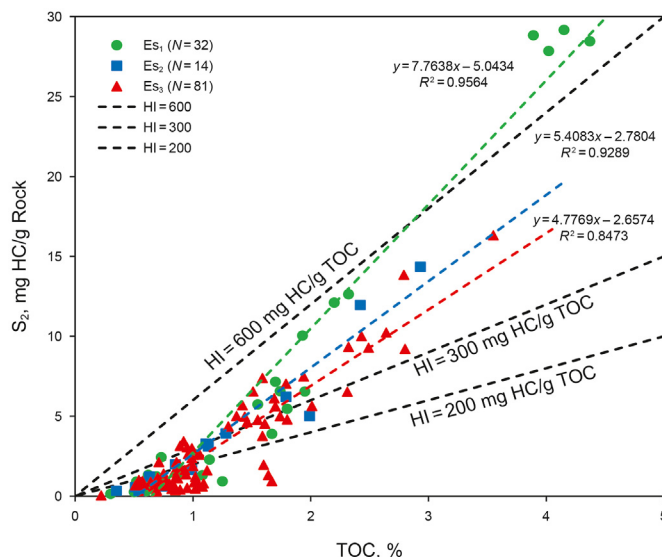


Fig. 6. TOC versus S_2 plot showing the kerogen types of the mudstones. N = number of samples.

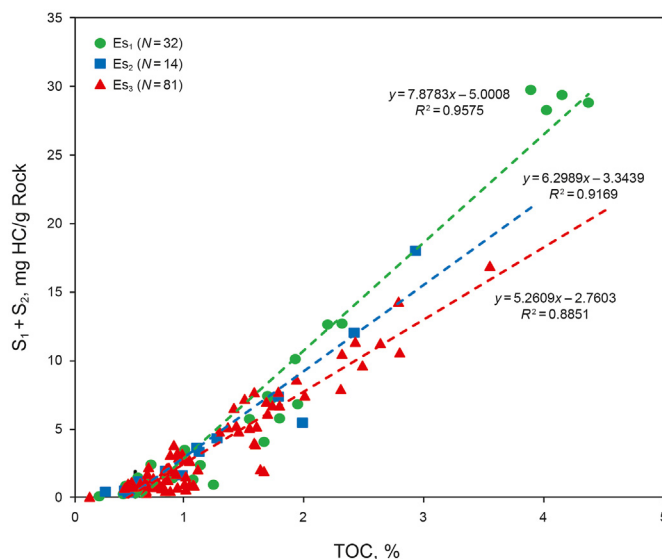


Fig. 7. TOC versus ($S_1 + S_2$) plot showing that the mudstones are mainly fair-good source rocks. N = number of samples.

4.2.4. Aromatic hydrocarbons

In mudstone samples, abundant alkylnaphthalenes, alkylphenanthrenes, dibenzothiophenes (DBT), dibenzofuran (DBF), and fluorene (F) were detected. DBT/phenanthrene (DBT/P) was believed to be related to redox conditions, and the ratio is very low in the samples, ranging from 0.01 to 0.05. The ternary plot of DBT, DBF, and F, which had been proposed by Lin et al. (1987), shows the paleoenvironment of sediments. There is a wide distribution of DBT range from 23.95% to 92.65%, as $DBT/(DBT + F + DBF)$ ratio reveals. $F/(DBT + F + DBF)$ and $DBF/(DBT + F + DBF)$ ratios are ranging from 0 to 23.13% and from 2.78% to 69.59%, respectively.

5. Discussion

5.1. Organic matter (OM) type and thermal maturity

What's generation of source rocks is determined by the OM type

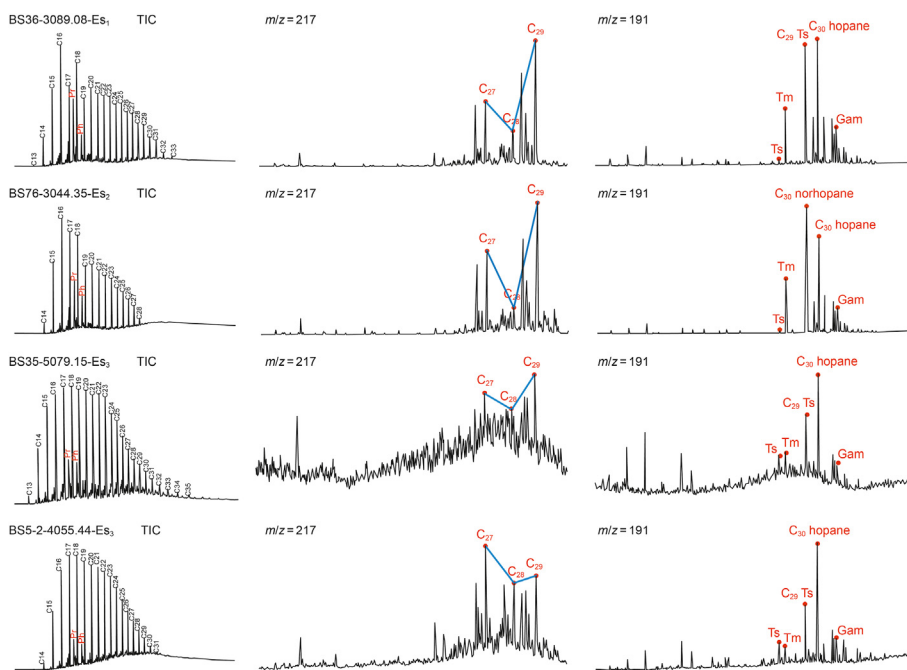


Fig. 8. The total ion chromatograms (TIC) (left), $m/z = 217$ (middle) and $m/z = 191$ (right) ion fragmentograms for some mudstones in Shahejie Formation of Banqiao Sag, Bohai Bay Basin. In the TIC fragmentograms, Pr = pristane, Ph = phytane; in the $m/z = 191$ fragmentograms, Ts = 18 α (H)-22,29,30-Trisnorhopane, Tm = 17 α (H)-22,29,30-Trisnorhopane, C₂₉Ts = 18 α (H)-30-Norhopane; Gam = Gammacerane; in the $m/z = 217$ fragmentograms, C₂₇, C₂₈, C₂₉ = C₂₇, C₂₈ and C₂₉ $\alpha\alpha\alpha$ 20R steranes.

(Tissot and Welte, 1978), which can be evaluated by the organic type index (TI) and the Rock-Eval pyrolysis hydrogen index (HI = 100 × S₂/TOC, mg HC/g TOC) (Espitalié, 1986; Peters, 1986).

Vitrinite and liptinite are the main maceral composition of the source rocks, mainly as collinite, telinite, vitrodetrinite and exodetrinite, suggesting that the main biological source is terrestrial plant tissues. The organic type index (TI) formula can be calculated to determine the OM type as following:

$$TI = \{Alginite \times (+100)liptinite \times (+50) + vitrinite(-75) + inertinite \times (-100)\} / 100$$

According to $TI > 80$, 40–80, 0–40, < 0, kerogens are divided into types I, II₁, II₂, and III. From most of the negative TI values, it can be seen that most of the samples are humic (type III), which is prone to gas generation, except two TI values of the samples belong to 0–40.

According to the wide variation in hydrogen indices, the studied samples show wide variations in kerogen types (Fig. 9). The source rocks in Es₃ are mainly mixed type II and III kerogen, indicated by relatively low hydrogen index.

While in Es₁, kerogen distributed from type I to type III, and this means the source of OM was a mixture of bacterial, algal, and higher plants, and higher plants making significant contributions in some part of the Banqiao Sag.

Through the n-alkane distribution patterns of saturated hydrocarbons, we determine the relative contribution of terrigenous versus aquatic OM to the sediments. The characteristic biomarkers of terrestrial higher plants are the long-chain n-alkanes (>nC₂₁), whereas the algae and microorganisms are the short-chain n-alkanes (<nC₂₀). The low nC₂₀/nC₂₁ ratios (Table S2) suggest the short-chain n-alkanes less than long-chain n-alkanes, which also means the source of OM are terrestrial OM. This is consistent with the maceral compositions and HI data.

The thermal maturity of OM can be determined by the T_{max} values. According to the T_{max} values < 435 °C, 435–445 °C,

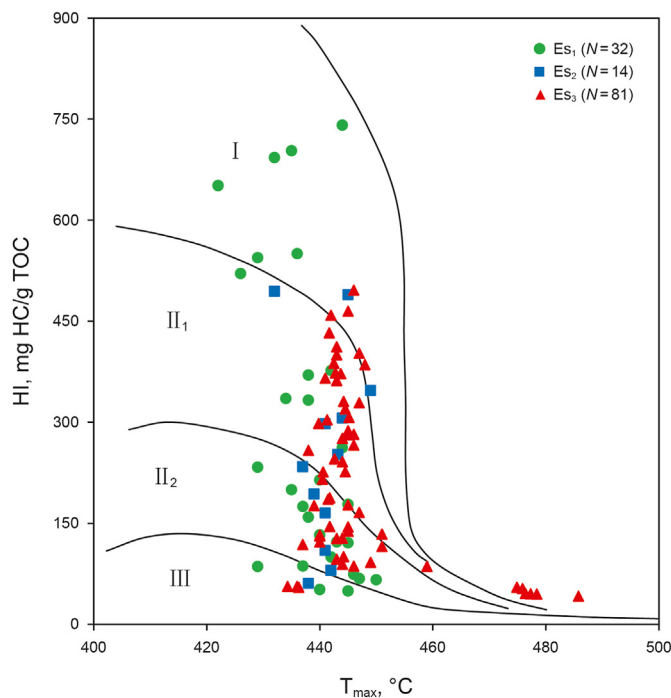


Fig. 9. The OM type classification diagram of HI- T_{max} . N = number of samples.

445–450 °C, 450–470 °C, > 470 °C, the OM are regarded to be immature, early, peak, late, or post mature, respectively. Based on this, the distribution of T_{max} values in most of the studied samples suggest a thermal maturity of early to late mature (Table S1, Fig. 10).

The low R_o samples from the Shahejie Formation (–0.41%–1.20%, lower than 1.30%) indicate that OM are mature and still in the oil window (Table S4). This is consistent with the conclusion drawn

from T_{max} values.

The C_{31} and C_{32} $22S/(22S + 22R)$ homohopane ratios are mostly close to the equilibrium values (0.57–0.62) (Table S3), indicating most of the samples are close to or exceeded the early mature stage. Similarly, the C_{29} and C_{30} $\alpha\beta/(\alpha\beta + \beta\alpha)$ hopane ratios (Table 1) are also close to the equilibrium value (around 0.9). On this basis, the OM have a slightly higher thermal maturity, but still suggestive of reaching the early oil generation window. In summary, the thermal maturity of mudstone samples, determined by $\alpha\beta/(\alpha\beta + \beta\alpha)$ hopane ratios and $22S/(22S + 22R)$ homohopane, is consistent with the R_o and T_{max} values.

When the OM reach peak oil generation and during early oil generation, the C_{29} $\alpha\beta\beta/(\alpha\beta\beta + \alpha\alpha\alpha)$ and C_{29} $\alpha\alpha\alpha$ $20S/(20S + 20R)$ sterane ratios are commonly stated as 0.67–0.71 and 0.52–0.55, respectively. The low to high C_{29} $\alpha\beta\beta/(\alpha\beta\beta + \alpha\alpha\alpha)$ and C_{29} $\alpha\alpha\alpha$ $20S/(20S + 20R)$ sterane ratios (0.16–0.60, 0.04–0.73), indicating the OM have low to high thermal maturity.

More than half of the mudstones are characterised by >1.0% TOC, and the OM are mainly type II₁ and II₂, and a low thermal maturity ($R_o < 1.3\%$), indicating that these rocks in Es Formation are effective oil and gas source rocks. Exploration indicates that the Banqiao Sag is rich in oil and gas and still has great potential for oil and gas discovery.

5.2. Source input and depositional environments

Carbon isotopes are mainly affected by sedimentary environment and the source of organic matter, minimally affected by maturity and transportation (Schoell, 1984; Zhang and Huang, 2005). The contribution of vegetable matter is often considered as an important factor leading to the enrichment of $\delta^{13}C$ in organic matter (Golyshev et al., 1991; Hofmann et al., 2000). The little difference in the distribution of $\delta^{13}C_{org}$ between Es₁ and Es₃ formations (Fig. 11). Most of the samples have $\delta^{13}C_{org}$ values higher than -27‰, except two of them in Es₁ formation lower than -27.7‰. The distribution of $\delta^{13}C_{org}$ show there are no apparent differences in the OM source among Shahejie Formation in Banqiao Sag. Higher aquatic plants accumulated and the contribution of terrestrial organic debris to sediments was significant in Es Formation.

The biological sources of organic matter are qualitatively analyzed based on the relative abundances of steranes, which are useful indicators to give an indication of source differences (Seifert and Moldowan, 1978; Huang and Meinschein, 1979). Huang and Meinschein(1979) proposed that C_{27} sterols are mainly derived

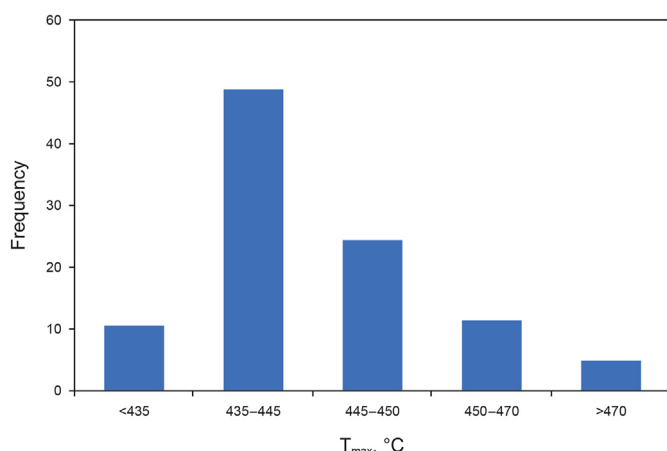


Fig. 10. Histograms of T_{max} in mudstones of the Shahejie Formation.

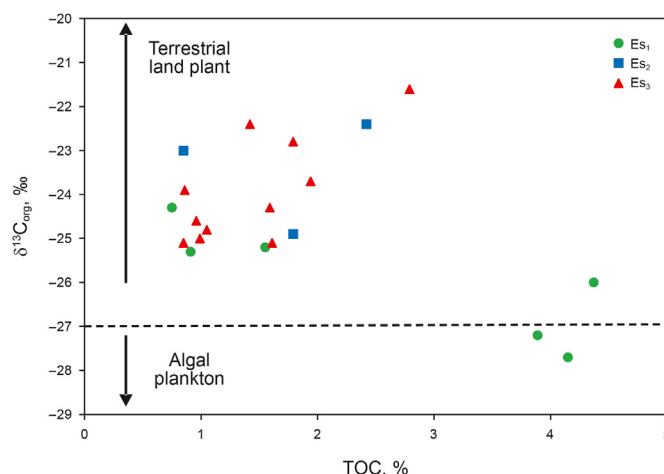


Fig. 11. Crossplot of the TOC versus carbon isotopic composition.

from algae, while C_{29} sterols are more typically associated with land plants. The low content of C_{28} sterols is typical of limnic environments indicated by Volkman (1986). The distributions of the steranes and diasteranes (C_{27} – C_{29}) can be seen from Fig. 8.

There is a low contribution of aquatic algal-bacterial OM and significant terrigenous OM input, because the samples have a higher proportion of C_{29} (21.16%–63.71%) compared to C_{27} (18.84%–62.92%) and C_{28} (10.91%–42.10%) steranes (Table S2), as indicated by regular steranes ternary diagram (Fig. 12).

On the whole, there are no apparent differences in the OM source among Shahejie Formation in Banqiao Sag. The proportional C_{29} sterane abundance in Es₁ is relatively higher than Es₃, which shows little more land plant input in Es₁. There is still plenty of planktic plant and bacterial in the source rocks from Es Formation (Fig. 12).

High C_{31} $22R$ homohopane/ C_{30} hopane ($C_{31R}/C_{30} > 0.25$) and C_{29}/C_{30} hopane (> 1.0) are generally indicative of carbonate or marl source rocks, but lower values are indicative of lacustrine source rocks. The studied samples of Es Formation in Banqiao Sag mainly

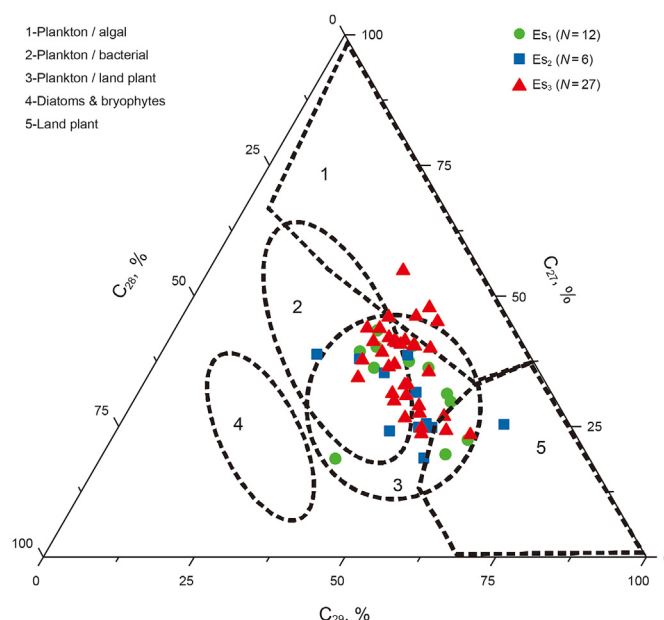


Fig. 12. Ternary diagram of regular steranes (C_{27} , C_{28} , and C_{29}).

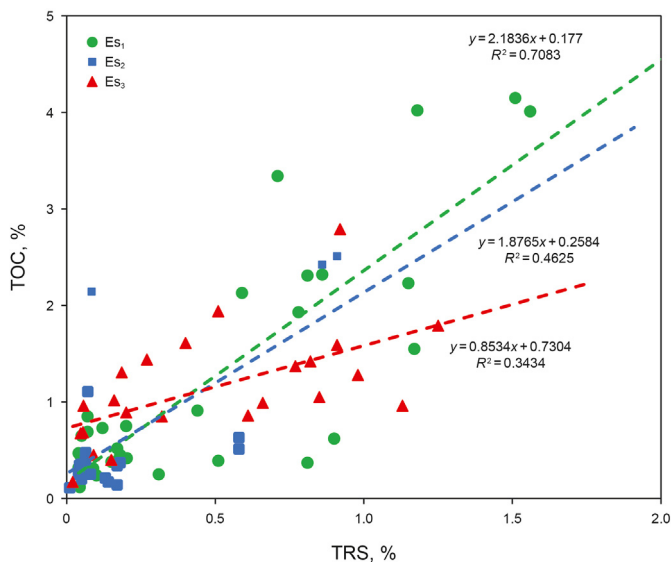


Fig. 13. Crossplot of the TRS versus TOC.

display low ratios of $C_{31}R/C_{30}$ (~0.05–0.31) and C_{29}/C_{30} hopane values (~0.06–1.36), indicating a lacustrine depositional environment (Table S3).

The redox conditions and sulfate concentration are commonly considered influencing the amount of total reduced sulfur (TRS) (Berner and Raiswell, 1984; Rao et al., 1994). The dissolved sulfate concentrations in lacustrine sediments are much lower than that in marine sediments (Berner and Raiswell, 1984), so the TRS can be used to indicate the redox conditions (Leventhal, 1983, 1995; Sampei et al., 1997; Mulier, 2002; Kao et al., 2004). The TRS lower than 0.2% is during oxidizing deposition, and over 0.4% is in an anoxic environment as well as ranging 0.2%–0.4% during suboxic deposition (Chen, 1987).

The TRS values in mudstone samples from Es₁ and Es₃ indicate a suboxic and anoxic environment, while most of the TRS values of mudstone samples from Es₂ formation are lower than 0.2%, indicating oxidizing depositional environment (Fig. 13).

The Pr/Ph ratios were commonly used to evaluate the depositional environments and organic matter source (Powell and

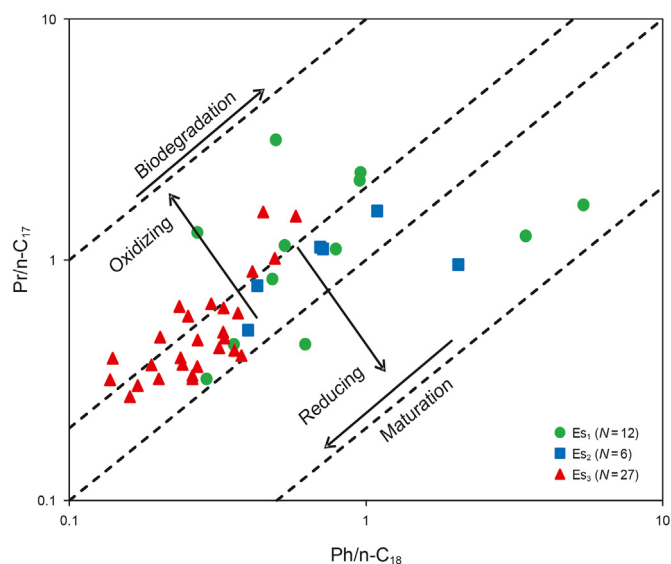


Fig. 14. Crossplot of Pr/n-C17 versus Ph/n-C18.

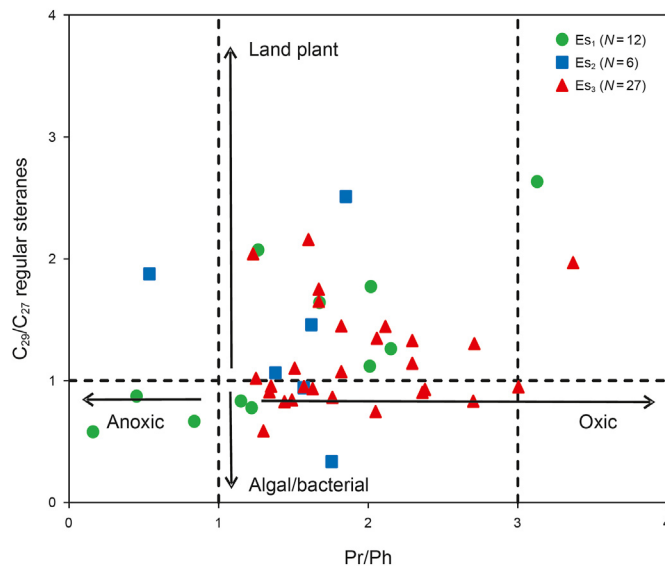


Fig. 15. Crossplot of C_{29}/C_{27} regular steranes versus Pr/Ph.

McKirdy, 1973; Didyk et al., 1978; Ten Haven et al., 1987; Hunt, 1996; Li et al., 1999; Harris et al., 2004; Hao et al., 2009). It is generally accepted that high Pr/Ph values (>3.0) suggest oxic environments and OM input of terrigenous. In contrast, low Pr/Ph values (<0.6) are commonly considered an argument for reducing and a highly saline depositional setting. The values of Pr/Ph show an extensive range (0.16–5.56) in the Shahejie Formation. The Shahejie Formation deposited in anoxic conditions, indicated by the low values in most of the samples (<3). Oxidizing and reducing environments are defined by Peters et al. (1999) through the plot of Pr/n-C₁₇ versus Ph/n-C₁₈ (Fig. 14). This plot supports mainly suboxic and weak reducing environments during the Es Formation deposited.

The cross plot of Pr/Ph versus C_{29}/C_{27} regular steranes can indicate the OM type and redox conditions of the sedimentary environment (Adegoke et al., 2014). The ratio of Pr/Ph between 0.16 and 5.56 and C_{29}/C_{27} regular steranes ratio are in the range of

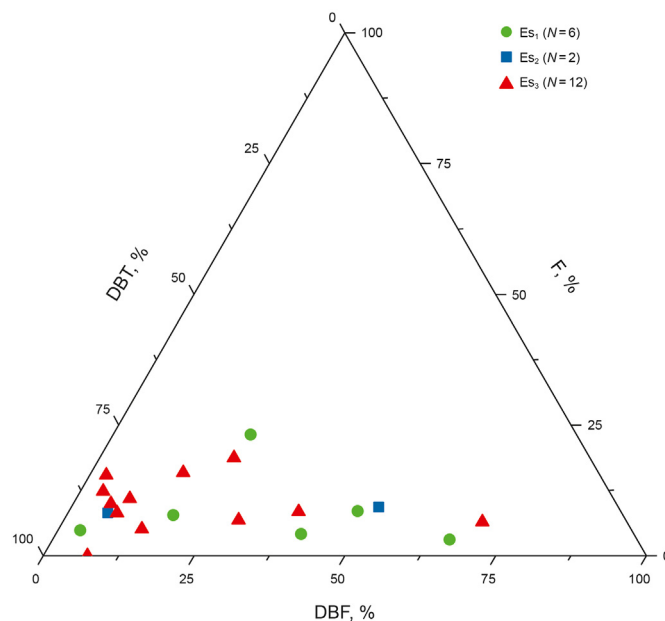


Fig. 16. Ternary diagram of F, DBT, and DBF.

0.34–2.89, indicating terrigenous organic matter and certain amount of bacteria preserved under suboxic to anoxic conditions (Fig. 15). Besides, the redox conditions of the sedimentary environment, suggested from several samples in Es₁, are nearly anoxic. The range of Pr/nC₁₇ and Ph/nC₁₈ ratios is more considerable in Es₁ than in Es₃. This would also be explained by the proportion of terrigenous OM and oxygen content in Es₁ being higher than that in Es₃ (Fig. 14).

The source rock extracts deposited under anoxic saline environments usually have low Pr/Ph ratios and high gammacerane index values, this means gammacerane can be an indicator of a salinity-stratified water column. The wide range of gammacerane index (1.99%–79.11%) and Pr/Ph ratios (0.16–5.56) indicate there is a great change of the sedimentary environment in Es Formation on time scale.

Due to the F, DBT, and DBF having similar molecular structure, they were derived from the same precursor. The relative component of F, DBT, and DBF is usually used to judge the primary depositional environment. The dominant DBF indicates oxic environment whereas abundant DBT was generally related to anoxic environments. According to Fig. 16, it can be concluded that most of the samples deposited in a reducing environment, which is also reflected in the cross plot of Pr/n-C₁₇ versus Ph/n-C₁₈.

6. Conclusion

Organic petrographic and geochemical results indicate that the Cenozoic Shahejie Formation mudstones in the Banqiao Sag, Bohai Bay Basin, China, generally have excellent oil and gas generation potential. The Cenozoic Shahejie Formation mudstones contain abundant OM with TOC values up to 4.37%. The analysis of maceral composition and biomarker indicate that the OM of the mudstones from Es Formation are type II and III kerogen. This conclusion is supported by its broad distribution of HI values, ranging from 18.18 to 741.13 mg HC/g TOC. The cross plot of Pr/n-C₁₇ versus Ph/n-C₁₈ indicate that the source rocks from Es Formation were deposited in a suboxic and weak reducing environment. In terms of hydrocarbon generation, the values of T_{max} , R_o , and biomarker maturity ratio indicate that the studied samples are at low to high mature stages. Abundant OM, type II and III kerogen, and moderate thermal maturity in most of the studied samples imply that they are effective oil and gas source rocks, and prove the potential for oil and gas exploration in the Banqiao Sag, Bohai Bay Basin is very good. This has been proven by the Cenozoic oil and gas found in the Banqiao area. These conclusions enhance the great prospect of oil and gas production in the Banqiao Sag.

Acknowledgements

This work was financially supported by the National Key Research and Development Program of China (Grant No. 2017YFC0603106). We appreciate the Petrochina Dagang Oilfield Company for providing background geologic data, samples and permission to publish this work. We also extend our appreciation to the editors and reviewers for their valuable and constructive comments and suggestions.

Appendix A. Supplementary data

Supplementary data to this article can be found online at <https://doi.org/10.1016/j.petsci.2022.07.002>.

References

Adegoke, A.K., Abdullah, W.H., Hakimi, M.H., et al., 2014. Geochemical

- characterisation of Fika formation in the Chad (Bornu) Basin, northeastern Nigeria: implications for depositional environment and tectonic setting. *Appl. Geochem.* 3, 1–12. <https://doi.org/10.1016/j.apgeochem.2014.01.008>.
- Bechtel, A., Jia, J., Strobl, S.A., et al., 2012. Palaeoenvironmental conditions during deposition of the Upper Cretaceous oil shale sequences in the Songliao Basin (NE China): implications from geochemical analysis. *Org. Geochem.* 46, 76–95. <https://doi.org/10.1016/j.orggeochem.2012.02.003>.
- Berner, R.A., Raiswell, R., 1984. C/S method for distinguishing freshwater from marine sedimentary rocks. *Geology.* 12, 365. [https://doi.org/10.1130/0091-7613\(1984\)12<365:CMFDF>2.0.CO;2](https://doi.org/10.1130/0091-7613(1984)12<365:CMFDF>2.0.CO;2).
- Brassell, S., Eglinton, G., Maxwell, J., 1978. *Natural Background of Alkanes in the Aquatic Environment*. Pergamon Press, Oxford, pp. 69–86. <https://doi.org/10.1016/B978-0-08-022059-8.50010-8>.
- Chen, J.Y., Wang, F.Y., 2010. Characteristics of source kitchen and hydrocarbon generation in Banqiao sag, bohaiwan basin. *Sci. Technol. Rev.* 28 (6), 78–82. <https://doi.org/10.1360/972009-1380> (in Chinese with English abstract).
- Chen, Z., 1987. *A Short Course of Petroleum Geology*. Geosciences Press, Beijing (in Chinese).
- Chen, G., Gang, W.Zh, Ch, X.Ch, et al., 2020. Paleoproductivity of the chang 7 unit in the ordos basin (north China) and its controlling factors. *Palaeogeogr. Palaeoclimatol. Palaeoecol.* 551, 109741. <https://doi.org/10.1016/j.palaeo.2020.109741>.
- Cheng, K.M., Wang, T.G., Zhong, N.N., 1995. *The Geochemistry of Source Rock*. Science Press, Beijing (in Chinese).
- Cheng, G.Y., Wang, X.P., Wang, T.G., et al., 1999. Compaction and primary hydrocarbon migration of immature source rocks in Banqiao Depression. *J. Jianghan Petroleum Inst.* 1 (1), 1–6 (in Chinese with English abstract).
- Damsté, J.S.S., Kenig, F., Koopmans, M.P., et al., 1995. Evidence for gammacerane as an indicator of water column stratification. *Geochem. Cosmochim. Acta.* 59 (9), 1895–1900. [https://doi.org/10.1016/0016-7037\(95\)00073-9](https://doi.org/10.1016/0016-7037(95)00073-9).
- Didyk, B., Simoneit, B., Brassell, S.C., et al., 1978. Organic geochemical indicators of palaeoenvironmental conditions of sedimentation. *Nature.* 272, 216–222. <https://doi.org/10.1038/272216a0>.
- Ding, X.J., Liu, G.D., Zha, M., et al., 2015. Characteristics and origin of lacustrine source rocks in the Lower Cretaceous, Erlian Basin, northern China. *Mar. Petrol. Geol.* 66, 939–955. <https://doi.org/10.1016/j.marpetgeo.2015.08.002>.
- Ding, X.J., Liu, G.D., Huang, ZhL., et al., 2016a. Source rock distribution and formation in Saihantala depression, Erlian Basin. *J. Cent. S. Univ.* 46 (5), 1739–1746. <https://doi.org/10.11817/j.jissn.1672-7207.2015.05.023> (in Chinese with English abstract).
- Ding, X.J., Liu, G.D., Zha, M., et al., 2016b. Geochemical characterization and depositional environment of source rocks of small fault basin in Erlian Basin, northern China. *Mar. Petrol. Geol.* 69, 231–240. <https://doi.org/10.1016/j.marpetgeo.2015.11.006>.
- Gao, G., Zhang, W.W., Xiang, B.L., et al., 2016. Geochemistry characteristics and hydrocarbon-generating potential of lacustrine source rock in Lucaogou formation of the Jimusaer sag, Junggar basin. *J. Petrol. Sci. Eng.* 145, 168–182. <https://doi.org/10.1016/j.petrol.2016.03.023>.
- Espitalié, J., 1986. Use of T_{max} as a maturation index for different types of organic matter – comparison with vitrinite reflectance. In: Burruss, J. (Ed.), *Thermal Modeling in Sedimentary Basins*. Editions Technip, Paris, Technip, pp. 475–496.
- Gao, G., Aderoju, Titi, Yang, ShR., et al., 2017. Geochemistry and depositional environment of fresh lacustrine source rock: a case study from the Triassic Baijiantan Formation shales in Junggar Basin, northwest China. *Org. Geochem.* 113, 75–89. <https://doi.org/10.1016/j.orggeochem.2017.08.002>.
- Golyshev, Stanislav I., Verkhovskaya, Natalia A., Burkova, Valentina N., et al., 1991. Matis. Stable carbon isotopes in source-bed organic matter of west and east siberia. *Org. Geochem.* 17 (3), 277–291. [https://doi.org/10.1016/0146-6380\(91\)90091-W](https://doi.org/10.1016/0146-6380(91)90091-W).
- Guo, X.W., He, Sh, Liu, K.Y., et al., 2011. Modelling the petroleum generation and migration of the third member of the Shahejie formation (Es3) in the Banqiao depression of Bohai bay basin, eastern China. *J. Asian Earth Sci.* 40, 287–302. <https://doi.org/10.1016/j.jseae.2010.07.002>.
- Hao, F., Zou, X.H., Zhu, Y.M., et al., 2009. Mechanisms of petroleum accumulation in the Bozhong sub-basin, Bohai Bay Basin, China. Part 1. Origin and occurrence of crude oils. *Mar. Petrol. Geol.* 26, 1528–1542. <https://doi.org/10.1016/j.marpetgeo.2008.09.005>.
- Harris, N.B., Freeman, K.H., Pancost, R.D., et al., 2004. The character and origin of lacustrine source rocks in the Lower Cretaceous synrift section, Congo Basin, West Africa. *Am. Assoc. Petrol. Geol. Bull.* 88, 1163–1184. <https://doi.org/10.1306/02260403069>.
- Hofmann, P., Ricken, W., Schwark, L., Leythaeuser, D., 2000. Carbon-sulfur-iron relationships and $\delta^{13}C$ of organic matter for late albian sedimentary rocks from the north atlantic ocean: paleoceanographic implications. *Palaeogeogr. Palaeoclimatol. Palaeoecol.* 163 (3), 97–113. [https://doi.org/10.1016/S0031-0182\(00\)00147-4](https://doi.org/10.1016/S0031-0182(00)00147-4).
- Huang, D.F., Li, J.Ch, Zhou, ZhH., et al., 1984. *Evolution and Hydrocarbon Generation Mechanism of Terrestrial Organic Matter*. Petroleum Industry Press, Beijing (in Chinese).
- Huang, W.Y., Meinschein, W.G., 1979. Sterols as ecological indicators. *Geochim.Cosmochim. Acta.* 43, 739–745. [https://doi.org/10.1016/0016-7037\(79\)90257-6](https://doi.org/10.1016/0016-7037(79)90257-6).
- Hughes, W.B., Holba, A.G., Dzou, L.I., 1995. The ratios of dibenzothiophene to phenanthrene and pristane to phytane as indicators of depositional environment and lithology of petroleum source rocks. *Geochem. Cosmochim. Acta.* 59 (17), 3581–3598. [https://doi.org/10.1016/0016-7037\(95\)00225-0](https://doi.org/10.1016/0016-7037(95)00225-0).

- Hunt, J.M., 1979. *Petroleum Geochemistry and Geology*. Freeman and Company, San Francisco, p. 524.
- Hunt, J.M., 1996. *Petroleum Geochemistry and Geology*. W.H. Freeman and Company, USA.
- Kao, S., Horng, C., Roberts, A.P., 2004. Carbon-sulfur-iron relationships in sedimentary rocks from southwestern Taiwan: influence of geochemical environment on greigite and pyrrhotite formation. *Chem. Geol.* 1, 153–168. <https://doi.org/10.1016/j.chemgeo.2003.09.007>.
- Leventhal, J.S., 1983. An interpretation of carbon and sulfur relationships in Black Sea sediments as indicators of environments of deposition. *Geochem. Cosmochim. Acta.* 47, 133–137. [https://doi.org/10.1016/0016-7037\(83\)90097-2](https://doi.org/10.1016/0016-7037(83)90097-2).
- Leventhal, J.S., 1995. Carbon-sulfur plots to show diagenetic and epigenetic sulfidation in sediments. *Geochem. Cosmochim. Acta.* 59, 1207–1211. [https://doi.org/10.1016/0016-7037\(95\)00036-Y](https://doi.org/10.1016/0016-7037(95)00036-Y).
- Li, M.W., Lin, R.Z., Liao, Y.S., et al., 1999. Organic geochemistry of oils and condensates in the Kekeya field, southwest depression of the Tarim Basin, China. *Org. Geochem.* 30 (1), 15–37. [https://doi.org/10.1016/S0146-6380\(98\)00201-0](https://doi.org/10.1016/S0146-6380(98)00201-0).
- Li, H.J., Wu, T.R., Ma, Z.J., et al., 2004. Pressure retardation of organic maturation in clastic reservoirs: a case study from the Banqiao Sag, eastern China. *Mar. Petrol. Geol.* 21 (9), 1083–1093. <https://doi.org/10.1016/j.marpetgeo.2004.07.005>.
- Lin, R.Z., Wang, P.R., Dai, Y.J., 1987. Petroleum geo-chemical significance of polycyclic aromatic hydrocarbons in fossil fuels. In: *Collection on Organic Geochemistry*. Geological Press, Beijing, pp. 129–140 (in Chinese).
- Liu, Q.X., Song, Y., Jiang, L., et al., 2017. Geochemistry and correlation of oils and source rocks in Banqiao Sag, Huanghua Depression, northern China. *J. Coal Geol.* 176–177, 49–68. <https://doi.org/10.1016/j.coal.2017.04.005>.
- Lu, S.F., Zhang, M., 2008. *Oil & Gas Geochemistry*. Petroleum Industry Press, Beijing (in Chinese).
- Luo, Q., George, S.C., Xu, Y., et al., 2016. Organic geochemical characteristics of the Mesoproterozoic Hongshuizhuang Formation from northern China: implications for thermal maturity and biological sources. *Org. Geochem.* 99, 23–37. <https://doi.org/10.1016/j.orggeochem.2016.05.004>.
- Mulier, A., 2002. Organic carbon burial rates, and carbon and sulfur relationships in coastal sediments of the southern Baltic Sea. *Appl. Geochem.* 17, 337–352. [https://doi.org/10.1016/S0883-2927\(01\)00087-7](https://doi.org/10.1016/S0883-2927(01)00087-7).
- Peters, K.E., 1986. Guidelines for evaluating petroleum source rock using programmed pyrolysis. *AAPG Bull.* 70, 318–329. <https://doi.org/10.1306/94885688-1704-11D7-8645000102C1865D>.
- Peters, K.E., Fraser, T.H., Amris, W., et al., 1999. Geochemistry of crude oils from eastern Indonesia. *AAPG Bull.* 83 (12), 1927–1942. <https://doi.org/10.1306/E4FD4643-1732-11D7-8645000102C1865D>.
- Peters, K.E., Walters, C.C., Moldowan, J.M., 2005. *The Biomarker Guide*. Cambridge University Press, Cambridge.
- Powell, T.G., McKirdy, D.M., 1973. Relationship between ratio of pristane to phytane in crude oil composition and geological environment in Australia. *Nature.* 243, 37–39. <https://doi.org/10.1038/physci243037a0>.
- Rao, P.S., Mascarenhas, A., Paropkari, A.L., et al., 1994. Organic carbon-sulfur relationships in sediment cores from the western and eastern continental margins of India. *Mar. Geol.* 117, 227–236. [https://doi.org/10.1016/0025-3227\(94\)90017-5](https://doi.org/10.1016/0025-3227(94)90017-5).
- Ren, Y.J., Lv, L., Liu, S., et al., 2014. Geochemical characteristics of light hydrocarbons in Banqiao Sag. *Nat. Gas Geosci.* 2014 25 (8), 1218–1225 (in Chinese with English abstract).
- Sampei, Y., Matsumoto, E., Kamei, T., et al., 1997. Sulfur and organic carbon-relationship in sediments from coastal brackish lakes in the Shimane peninsula-district, southwest Japan. *Geochem. J.* 31, 245–262. <https://doi.org/10.2343/geochemj.31.245>.
- Schoell, M., 1984. Recent advances in petroleum isotope geochemistry. *Org. Geochem.* 6, 645–663. [https://doi.org/10.1016/0146-6380\(84\)90086-X](https://doi.org/10.1016/0146-6380(84)90086-X).
- Seifert, W.K., Moldowan, J.M., 1978. Applications of steranes, terpanes and monoaromatics to the maturation, migration and source of crude oils. *Geochem. Cosmochim. Acta* 42, 77–95. [https://doi.org/10.1016/0016-7037\(78\)90219-3](https://doi.org/10.1016/0016-7037(78)90219-3).
- Song, F., Su, N.N., Li, H., et al., 2015. Structural characteristics and hydrocarbon accumulation model of Dazhangtuo fault belt in the Banqiao Sag. *J. NE. Petrol. Univ.* 39 (6), 12–19 (in Chinese with English abstract).
- Sun, Ch, Hou, D.J., Zhang, X.T., et al., 2012. The geochemical characteristics and its genesis of some of the oils from Banqiao-Beidagang. *J. Oil Gas Technol. (J. Jiangnan Petroleum Inst.)* 34 (11), 26–30 (in Chinese with English abstract).
- Ten Haven, H.L., De Leeuw, J.W., Rullkötter, J., et al., 1987. Restricted utility of the pristane/phytane ratio as a palaeoenvironmental indicator. *Nature.* 330 (6149), 641–643. <https://doi.org/10.1038/330641a0>, 1987.
- Tissot, B.P., Welte, D.H., 1978. *Petroleum Formation and Occurrence*. Springer Verlag, Berlin, Heidelberg, New York.
- Volkman, J.K., 1986. A review of sterol biomarkers for marine and terrigenous organic matter. *Org. Geochem.* 9, 83–89. [https://doi.org/10.1016/0146-6380\(86\)90089-6](https://doi.org/10.1016/0146-6380(86)90089-6).
- Wang, M., Sherwood, N., Li, Z.S., et al., 2015. Shale oil occurring between salt intervals in the Dongpu depression, Bohai bay basin, China. *Int. J. Coal Geol.* 152, 100–112. <https://doi.org/10.1016/j.coal.2015.07.004>.
- Yang, J.L., Shang, H.G., Hu, Q.Y., 2019. Organic geochemical characteristics of crude oils from Banqiao depression, Bohai bay basin. *J. Shengli Coll. China Univ. Petrol.* 33 (4), 10–17 (in Chinese).
- Zhang, S.C., Huang, H.P., 2005. Geochemistry of palaeozoic marine petroleum from the Tarim basin, NW China. Part 1. *Org. Geochem.* 36, 1204–1214. <https://doi.org/10.1016/j.orggeochem.2005.01.013>.
- Zhang, G.Q., Li, Y.F., He, Sh, et al., 2009. Composition characteristics and geochemical significance of aromatic hydrocarbons of crude oils from the Banqiao Depression. *Acta Sedimentol. Sin.* 27 (2), 367–371 (in Chinese with English abstract).
- Zhao, X.Zh, Liu, G.D., Jin, F.M., 2015. Distribution features and pattern of effective source rock in small faulted lacustrine basin: a case study of the Lower Cretaceous in Erlian Basin. *Acta Pet. Sin.* 36 (6), 641–652 (in Chinese with English abstract).